Original Article

Kurume Medical Journal, 69, 237-249, 2022

Comprehensive Molecular Profiling and Clinicopathological Characteristics of Gastric-Type Mucinous Carcinoma of the Uterine Cervix in Japanese Women

HIROKI NASU*, SHIN NISHIO*, JONGMYUNG PARK*, KAZUTO TASAKI*, ATSUMU TERADA*, NAOTAKE TSUDA*, KOUICHIRO KAWANO‡, SAKIKO KOJIRO-SANADA**, JUN AKIBA† AND KIMIO USHIJIMA*

**Department of Obstetrics and Gynecology,*
***Department of Pathology, Kurume University School of Medicine,*
†Department of Diagnostic Pathology, Kurume University Hospital, Kurume 830-0011,
‡Kawano Ladies Clinic, Fukuoka 813-0044, Japan

Received 8 October 2022, accepted 27 December 2022
J-STAGE advance publication 16 February 2024

Edited by YOSHITO AKAGI

Summary: Gastric-type mucinous carcinoma (GAS) of the uterine cervix is the most common adenocarcinoma that develops independently of human papillomavirus infection; it is typically diagnosed at an advanced stage and has a poorer prognosis than usual-type endocervical adenocarcinoma. Few studies have examined the molecular profile of GAS, but genetic alterations in *TP53* and *STK11* have been repeatedly reported. We analyzed the clinicopathological characteristics and molecular profile of GAS. Fresh-frozen tissue specimens and formalin-fixed paraffin-embedded (FFPE) tissues from 13 patients with GAS treated between January 2000 and December 2020 were analyzed. We performed next-generation sequencing on eight fresh-frozen GAS specimens using the Cancer Hotspot Panel v2 (cases 1–8) and the FoundationOne companion diagnostic (F1CDx) assay on six FFPE samples (cases 8–13). Seventy-four genomic alterations were identified in 42 genes. In order of frequency, *TP53*, *ATRX*, *CDKN2A*, *KRAS*, *APC*, and *STK11* were altered in at least three cases. Targetable genomic alterations were identified in all six patients' specimens analyzed using the F1CDx assay. GAS harbors various genomic alterations associated with sustained activation of signaling pathways or cell cycle regulation in addition to abnormalities in *TP53*, and precision medicine based on molecular profiling will be necessary to overcome GAS.

Keywords gastric-type mucinous carcinoma, high-throughput nucleotide sequencing, human papillomavirus, immunohistochemistry, uterine cervical neoplasms

INTRODUCTION

Histopathology and epidemiology

Gastric-type mucinous carcinoma (GAS) of the uterine cervix is an aggressive variant of endocervical adenocarcinoma (ECA), which was newly described in the 2014 World Health Organization classification [1]. Kojima et al. defined GAS as a mucinous carcinoma consisting of cells with a voluminous clear or pale eosinophilic cytoplasm and distinct borders [2]. GAS

Corresponding Author: Hiroki Nasu, M.D., Department of Obstetrics and Gynecology, Kurume University School of Medicine, 67 Asahi-machi, Kurume, Fukuoka 830-0011, Japan. Tel: +81-942-31-7573, Fax: +81-942-35-0238, E-mail: nasu_hiroki@kurume-u.ac.jp

Abbreviations: COSMIC, Catalog of Somatic Mutations in Cancer; ECA, endocervical adenocarcinoma; FDA, Food and Drug Administration; FFPE, formalin-fixed paraffin-embedded; gAIS, gastric-type adenocarcinoma in situ; GAS, gastric-type mucinous carcinoma; HPV, human papillomavirus; IHC, immunohistochemistry; ISP, ion sphere particle; LEGH, lobular endocervical glandular hyperplasia; MBRT, molecular-based recommended therapy; MMR, mismatch repair; HRD, homologous recombination deficiency; MSI, microsatellite instability; NGS, next-generation sequencing; OS, overall survival; PCR, polymerase chain reaction; PFS, progression-free survival; SCTAT, sex cord tumor with annular tubules; TGA, targetable genomic alteration; TMB, tumor mutational burden; UEA, usual-type endocervical adenocarcinoma.

involves gastric differentiation and is positive for HIK1083 and/or MUC6 expression [3]. Immunohistochemically, GAS is negative for p16 and shows an aberrant p53 pattern [3,4]. GAS accounts for 20–25% and 1.7% of cases of ECA in Japan and Western countries, respectively, with some regional differences [2,5,6].

Clinical and biological characteristics

GAS tends to be diagnosed at an advanced stage, with frequent lymph node metastasis, ovarian involvement, peritoneal dissemination, and distant metastases [7]. GAS has been reported to have a much poorer prognosis than usual-type endocervical adenocarcinoma (UEA), even when matched by stage [8]. In addition to its aggressive nature, chemotherapy and radiotherapy resistance may contribute to a poor prognosis [8,9]. Unlike UEA, GAS is not associated with high-risk human papillomavirus (HPV) infection [5].

Distinct genetic alterations

Several studies investigating the GAS molecular profile using next-generation sequencing (NGS) have reported recurrent and common genetic variants in *TP53*, *CDKN2A*, *KRAS*, and *STK11* [10–15]. However, genetic alterations underlying the aggressiveness of GAS and HPV-independent carcinogenesis have not been characterized. Furthermore, despite the high prevalence of GAS in Japan, representative studies are limited to a multicenter, large-scale clinical pathological report; no studies have yet used NGS [8].

Study purpose

We performed NGS using fresh-frozen and formalin-fixed paraffin-embedded (FFPE) specimens of GAS in the Japanese population and examined the relationship between the clinicopathological features and molecular profile of GAS. This study aimed to understand the molecular pathogenesis of GAS and aid the development of new therapeutic strategies using precision medicine.

MATERIALS AND METHODS

Study population and sample collection

The study population comprised patients with GAS treated in our institution between January 2000 and December 2020. Surgically treated patients whose fresh-frozen tumor specimens were available were originally included. However, the availability of fresh frozen samples in clinical practice is limited due to its high cost and technical difficulty, making the accumulation of cases difficult. Thus, to increase the sample size, patients who underwent comprehensive genomic profiling for F1CDx were also included after approval from the Japanese National Health Insurance system for patients with solid tumors refractory to standard care in May 2019. Representative hematoxylin-eosin-stained slides were reviewed by a gynecological pathologist (S.K.-S.). All procedures involving human participants were in accordance with the 1964 Declaration of Helsinki and its later amendments. The study protocol was approved by the Ethics Committee of Kurume University (study ID: 387). Informed consent was obtained from all participants included in the study.

Clinicopathological data collection

The patients' clinicopathological parameters were obtained from their medical records and included age, clinical manifestation, International Federation of Gynecology and Obstetrics 2018 stage, surgery type, adjuvant therapy, follow-up, clinical outcome, HPV status, and pathological findings. Deep stromal invasion was defined as invasion of the outer one-third of the cervical stroma. Progression-free survival (PFS) was defined as the time from the first date of treatment to disease progression or death, and overall survival (OS) was defined as the time from the first date of treatment to death.

Targeted sequencing assay

Fresh frozen tissue specimens from eight patients were examined with targeted sequencing. Genomic DNA was isolated from fresh-frozen tissue samples using the AllPrep DNA/RNA/Protein Mini Kit (QIAGEN, Hilden, Germany) according to the manufacturer's protocol. For each sample, 10 ng of DNA was used to prepare sequencing libraries. The target regions of DNA were amplified from the Ion AmpliSeq Library Kit 2.0 (Thermo Fisher Scientific, Waltham, MA, USA) using the Ion Cancer Hotspot Panel v2 (CHPv2, Thermo Fisher Scientific, Waltham, MA, USA) following the manufacturer's instructions. CHPv2 is composed of 207 amplicons, covering 2,790 Catalog of Somatic Mutations in Cancer (COSMIC) mutations from 50 oncogenes and tumor-suppressor genes: *ABL1, AKT1, ALK, APC, ATM, BRAF, CDH1, CDKN2A, CSF1R, CTNNB1, EGFR, ERBB2, ERBB4, EZH2, FBXW7, FGFR1, FGFR2, FGFR3, FLT3, GNA11, GNAQ, GNAS, HNF1A, HRAS, IDH1, IDH2, JAK2, JAK3, KDR, KIT, KRAS, MET, MLH1, MPL, NOTCH1, NPM1, NRAS, PDGFRA, PIK3CA, PTEN,*

PTPN11, RB1, RET, SMAD4, SMARCB1, SMO, SRC, STK11, TP53, and *VHL*. Barcoded libraries were generated from the amplicons using the Ion Xpress Barcode Adapters Kit (Thermo Fisher Scientific, Waltham, MA, USA). Libraries were amplified using Platinum PCR SuperMix High Fidelity (Thermo Fisher Scientific, Waltham, MA, USA) and quantified using the Agilent 2100 Bioanalyzer instrument and Agilent High Sensitivity DNA Kit (both from Agilent, Santa Clara, CA, USA). Eight barcode libraries were combined in a pooled library for automated template preparation using the Ion Chef System and the Ion 520 & 530 Kit – Chef (Thermo Fisher Scientific, Waltham, MA, USA). The mixed library was clonally amplified on ion sphere particles (ISP) in a water-oil emulsion and the enriched ISPs were loaded onto an Ion 530 chip (Thermo Fisher Scientific, Waltham, MA, USA) according to the manufacturer's instructions. Sequence analysis was performed using the Ion S5 system.

Bioinformatics

We used Torrent Suite software (version 5.2.0, Thermo Fisher Scientific, Waltham, MA, USA) to sequence genes. After alignment to the reference genome (hg 19: *Homo sapiens*), genetic variants were identified using the Ion Torrent Variant Caller plug-in version 5.2.0, and annotation was performed using the Ion Reporter software. Frameshift variants were determined to be abnormal. Common single-nucleotide polymorphisms, synonymous variants, and variants reported as benign or likely benign in the ClinVar database (http://www.ncbi.nlm.nih.gov/clinvar/) were removed. In cases where there was no significant information available in ClinVar, the Leiden Open Variation Database (http://www.lovd.nl/3.0/home) was referenced.

Comprehensive genomic profiling assay

The F1CDx assay was performed in six patients with refractory disease using FFPE samples [16]. For one patient, both the CHPv2 and F1CDx assays were performed. F1CDx detects substitutions, insertion/deletion alterations (indels), and copy number alterations in 324 genes, selected gene rearrangements, and genomic signatures, including microsatellite instability (MSI) and tumor mutational burden (TMB), using DNA extracted from FFPE specimens. TMB-high was defined as 10 or more mutations per megabase. Each result in the F1CDx report was carefully assessed by the institutional molecular tumor board, which consisted of a multidisciplinary team of medical oncologists, surgeons, medical geneticists, genetic counselors, pharmacists, pathologists, and basic scientists for molecular-based recommended therapies (MBRT). We defined targetable genomic alterations (TGA) according to the OncoKB therapeutic level of evidence V2 with four categories (http://oncokb.org): Level 1: Food and Drug Administration (FDA)-recognized biomarker predictive of response to an FDA-approved drug in this indication; Level 2: standard care biomarker predictive of response to an FDA-approved drug in this indication; Level 3: compelling clinical evidence supports the biomarker as being predictive of response to a drug in this indication (3A) or standard care or investigational biomarker predictive of response to an FDA-approved or investigational drug in another indication (3B); and Level 4: compelling biological evidence supports the biomarker as being predictive of response to a drug in other indications.

Immunohistochemistry

Immunohistochemistry for p16, p53, and other relevant protein markers was performed to support the diagnosis and complement the molecular analysis. Paraffin-embedded tissue samples were cut into 4-μm sections and labeled using BenchMark XT (Ventata Automated Systems Inc., Tucson, AZ, USA) with tumor antigen antibodies. The iVIEW DAB Detection Kit (Ventana Medical Systems, Inc., Oro Valley, AZ, USA) was used for the detection of antigens as previously described [17]. The primary antibodies used for immunohistochemistry (IHC) were a monoclonal mouse antihuman β-catenin antibody (catalog #M353901-2; Agilent Technologies, Santa Clara, CA, USA), monoclonal mouse anti-p53 antibody (catalog # P53-DO7-L-CE; Leica Biosystems, Wetzlar, Germany), and a monoclonal mouse anti-p16 antibody (catalog # 705-4713 CINtec p16 Histology; Roche, Basel, Switzerland). The p53 immunostaining pattern was evaluated as having normal (10–50% cells stained) or abnormal expression, which was defined as either overexpression (60–100% of positive cells) or complete absence (0% of positive cells). The p16 immunostaining pattern was categorized as positive if all tumor cells were diffuse and had strong nuclear and cytoplasmic staining, while no staining or patchy staining was categorized as negative.

HPV detection and genotyping

HPV tests were performed using liquid-based cytology samples (ThinPrep; Hologic, Marlborough, MA, USA) collected by scraping the tumor surface with a cytobrush. The GENOSEARCH HPV 31 kit

(Medical and Biological Laboratory, Nagoya, Japan) was used for the detection and identification of 31 HPV genotypes, including high- (16, 18, 31, 33, 35, 39, 45, 51, 52, 56, 58, 59, and 68) and low-risk types (6, 11, 26, 42, 44, 53, 54, 55, 61, 62, 66, 70, 71, 73, 82, 84, 90, and CP6108) using reverse sequence-specific oligonucleotide polymerase chain reaction (PCR) [18]. Briefly, DNA was amplified using multiplex PCR. The resulting amplicon mixtures were hybridized with genotype-specific probes, which were detected using the Luminex System (Luminex, Austin, TX, USA). ß-globin was used as an internal control to verify the presence of sufficient cellular components in the samples.

RESULTS

Patient characteristics

In total, 13 patients were included in this study. The median age at the time of diagnosis was 50 years (range 38-77). The most common clinical manifestation was atypical genital bleeding (6/13, 46.2%), followed by lower abdominal pain (3/13, 23.1%). Ten of the 13 patients had an abnormal cervical pap smear result, including "adenocarcinoma" in nine patients and "atypical glandular cells" in one patient. All patients were diagnosed with adenocarcinoma or GAS by cervical biopsy or endocervical curettage, none of which detected human papillomavirus DNA, except patient 13, who was positive for HPV 52. The characteristics of patients with GAS are shown in Table 1. The typical histology of GAS in our cases is shown in Figure 1.

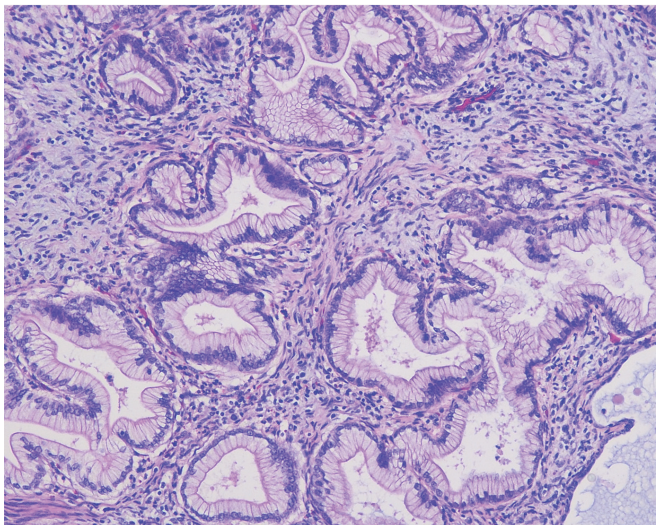

Fig. 1. Gastric-type mucinous carcinoma (hematoxylin and eosin). Neoplastic glands composed of cells with voluminous clear or pale eosinophilic cytoplasm and distinct borders.

The most common clinical stage at the time of presentation was ⅢC (7/13, 53.8%), followed by IVB (3/13, 23.1%). Radical abdominal hysterectomy, modified radical hysterectomy, and total abdominal hysterectomy were performed in four cases each, and heavy-ion radiotherapy was administered in the remaining case. Bilateral salpingo-oophorectomy was performed in all cases except case 12, in which heavy-ion radiotherapy was administered. All patients treated with surgery, except case 9, received adjuvant chemotherapy or radiotherapy. Ten patients had lymph node metastases, and 11 patients had extracervical extension, including the ovary (5/13, 38.5%), vagina (4/13, 30.8%), parametrium (3/13, 23.1%), and peritoneum (3/13, 23.1%). Among the 12 patients who underwent surgery, there was lymphovascular space invasion in 11 and deep stromal invasion was identified in 10. Seven of the 13 patients (53.9%) died from the disease, and one of the 13 (7.7%) patients was alive with no evidence of the disease at the data collection cutoff date of January 31, 2022. One patient was lost to follow-up and censored on the last date of examination. The median PFS and OS were 8.1 and 20.2 months, respectively. In nine patients, there was a family history of malignancy. The family history breakdown included uterine (n = 2), pancreatic (n = 2), breast (n = 1), colorectal (n = 1), gastric (n = 1), liver (n = 1), lung (n = 1), renal (n = 1), and tongue (n = 1) cancers, as well as malignant mediastinal tumor (n = 1), malignant melanoma (n = 1), and soft tissue sarcoma (n = 1). None of the patients had a medical or family history suggestive of Peutz–Jeghers syndrome (PJS), but case 8 presented coexisting minimal deviation adenocarcinoma (MDA) and ovarian sex cord tumor with annular tubules (SCTAT), which could be associated with PJS.

Molecular profiling

Targeted sequencing using CHPv2 was performed in cases 1–8. Comprehensive genomic profiling with F1CDx was performed in cases 8–13. In case 8, relapse occurred after the CHPv2 assay, and F1CDx was subsequently performed, resulting in analysis with both assays. In the CHPv2 assay, the average number of mapped reads per sample was 632,449 (range, 486,801–799,168), the on-target coverage was 94.7%, and the base coverage depth was 2,850 (range, 2,207–3,613). A total of 74 alterations were identified in 42 genes. The breakdown is as follows: In the CHPv2 assay (cases 1–8), we identified 15 variants among 6 different genes, including *TP53* (6/8, 75.0%), *APC* (3/8, 37.5%), *PIK3CA* (2/8, 25.0%), *CDKN2A* (2/8, 25.0%),

TABLE 1.
Patient clinicopathological characteristics

Case	Age at Dx, years	Clinical manifestation	Pap smear result	Histological Dx	Stage at presentation (FIGO 2018)	T	N	M	Extracervical extension	Treatment		Follow-up, months	Status
										Main	Adjuvant		
1	50	Abdominal distension	Adenocarcinoma	Adenocarcinoma	IB1	1b1	0	0	Ovary	TAH	RT	8	DOD
2	57	Lower abdominal pain	Adenocarcinoma	Adenocarcinoma	IIIC2	2b	2	0	Parametrium	mRH	RT	15	DOD
3	53	Atypical genital bleeding	Adenocarcinoma	Adenocarcinoma	IIIC1	1b1	1	0	None	RH	RT	45	LTF
4	44	Lower abdominal pain	Adenocarcinoma	Adenocarcinoma	IVB	4	1	1	Ovary, Peritoneum	TAH	CT	1	DOD
5	40	Atypical genital bleeding	Adenocarcinoma	Adenocarcinoma	IIIC1	2a2	1	0	Ovary, vagina	RH	CT	14	DOD
6	40	Abnormal vaginal discharge	NILM	AIS	IIA1	2a1	0	0	Vagina	RH	CT	75	NED
7	70	Atypical genital bleeding	NILM	Adenocarcinoma	IVB	4	1	1	Parametrium, Peritoneum	mRH	CT	4	DOD
8	38	Lower abdominal pain	AGC	GAS	IIIC1	1b2	1	0	Ovary	RH	CT	51	AWD
9	75	N/A	N/A	N/A	IA1	1a1	0	0	None	TAH	None	36	AWD
10	70	Abdominal distension	Adenocarcinoma	Adenocarcinoma	IVB	4	1	1	Ovary, Peritoneum	TAH	CT	21	DOD
11	42	Atypical genital bleeding	Adenocarcinoma	GAS	IIIC2	2a2	2	0	Vagina	mRH	CT	13	DOD
12	41	Atypical genital bleeding	Adenocarcinoma	GAS	IIIC1	2a2	1	0	Vagina	HIR	None	4	AWD
13	77	Atypical genital bleeding	Adenocarcinoma	GAS	IIIC1	2b	1	0	Parametrium	mRH	CT	24	AWD

Abbreviations: Dx, diagnosis; FIGO, International Federation of Gynecology and Obstetrics; N/A, not available; NILM, negative for intraepithelial lesion or malignancy; AGC, atypical glandular cells; AIS, adenocarcinoma in situ; GAS, gastric-type mucinous carcinoma; TAH, total abdominal hysterectomy; mRH, modified radical hysterectomy; RH, radical hysterectomy; HIR, heavy-ion radiotherapy; RT, radiation therapy; CT, chemotherapy; DOD, died of disease; LTF, lost to follow-up; NED, no evidence of disease; AWD, alive with disease.

KIT (1/8, 12.5%), and *KRAS* (1/8, 12.5%), using the filtering criteria mentioned above, while in the F1CDx assay (cases 8–13), 60 alterations were identified between 39 genes, including *CDKN2A* (5/6, 83.3%), *KRAS* (4/6, 66.7%), *ATRX* (3/6, 50.0%), *STK11* (3/6, 50.0%), *TP53* (3/6, 50.0%), *DAXX* (2/6, 33.3%), *ERBB2* (2/6, 33.3%), *RNF43* (2/6, 33.3%), *ROS1* (2/6, 33.3%), and *TGFBR2* (2/6, 33.3%). In case 8, an alteration in *CDKN2A* was identified in both CHPv2 and F1CDx, while alterations in the other eight genes were detected only in the F1CDx assay. All 13 patients showed one or more alterations (range, 1–14). Combining the analyzes by the CHPv2 and F1CDx assay, the gene most frequently altered was *TP53* (9/13, 69.2%), followed by *ATRX* (3/6, 50%), *CDKN2A* (5/13, 38.5%), *KRAS* (5/13, 38.5%), *APC* (3/13, 23.1%), and *STK11* (3/13, 23.1%). The gene with the highest number of alterations was *TP53* (9), followed by *CDKN2A* (7), *KRAS* (6), *APC* (3) *STK11* (3), and *ATRX* (3). The results of molecular profiling are summarized in Figure 2 and Table 2. The distribution of altered genes classified by variant type is shown in Figure 3 for F1CDx and Supplementary Figure 1S for CHPv2.

Among the six patients (cases 8–13) analyzed using the F1CDx assay, TGAs were observed in six (9/9, 100%), all of which were Level 3B or 4. There were no MSI-high or TMB-high tumors. The molecular tumor board did not propose any MBRTs. The breakdown of TGA included oncogenic mutations of *CDKN2A* (n = 5), *KRAS* (n = 3), and *ERBB2* (n = 2), and a truncated mutation of *ARID1A* (n = 1).

TP53 was the gene most frequently altered, including seven missense variants, one frameshift variant, and one splice-site variant. IHC revealed p53 overexpression in seven cases of missense variants and one case of a splice-site variant, while expression was completely absent in one case of a frameshift variant and one case of no significant variants (Figures 4A, B). The *CDKN2A* alterations included three nonsense variants, two frameshift variants, one missense variant, and one intron rearrangement. In case 11, both the nonsense and frameshift variants in *CDKN2A* were observed. All *KRAS* alterations were missense variants, while *APC* alterations included two frameshift variants and one in-frame indel variant. Expression of nuclear β-catenin was negative in all eight cases in which immunostaining was performed (Figure 4C). Three *STK11* alterations were found, including one missense variant, one frameshift variant, and *STK11* loss. HPV genotyping results were negative, except in case 13, in which HPV 52 positivity was noted, and staining for p16 was negative in all the 11 cases where immunostaining was performed (Figure 4D). The relationship between molecular profiles and immunophenotype is shown in Table 3.

DISCUSSION

In this study, we reviewed the clinicopathological features and examined the molecular profile of GAS. Our clinical data are consistent with the previous literature showing HPV independence, high rates of lymph node metastasis, lymphovascular invasion, extracervical extension, and poor prognosis. We analyzed 13 GAS cases. Of these, targeted sequencing with CHPv2 was performed in eight cases, and comprehensive genomic profiling using F1CDx was performed in six cases. We identified 74 alterations in 42 genes, including *TP53, CDKN2A, KRAS, APC, ATRX, STK11, ARID1A, DAXX, ERBB2, PIK3CA, RNF43, ROS1*, and *TGFBR2*. With the exception of β-catenin, the immunohistochemical pattern of the expressed genes, including p53 and p16, was generally consistent with the molecular profile results.

The gene most commonly altered was *TP53*, followed by *CDKN2A, KRAS, APC, ATRX, STK11, ARID1A, DAXX, ERBB2, PIK3CA, RNF43, ROS1*, and *TGFBR2*. *TP53, CDKN2A, APC, ATRX, STK11, ARID1A, DAXX, RNF43*, and *TGFBR2* function as tumor-suppressor genes, while *KRAS, ERBB2, PIK3CA*, and *ROS1* are oncogenes.

As in previous reports, *TP53* variants were the most common, suggesting that *TP53* plays a vital role in GAS [10–12,15]. *TP53*, which is the most mutated gene in cancer, encodes p53 that regulates genes involved in cellular processes, including cell cycle arrest, DNA repair, and apoptosis, and is designated to have a canonical function. Most *TP53* alterations in cancers are missense variants that produce mutant p53 proteins, which commonly lose their tumor-suppressor function and acquire various gain-of-function activities that promote tumor development [19]. *TP53* variants were found in more than half of the cases in this study. Immunohistochemical staining revealed aberrant p53 expression in most cases, and negative staining for p16 in all cases, regardless of HPV presence. The missense and frameshift variants in *TP53* were associated with the overexpression and negative expression of p53, respectively, and the expression pattern was consistent with the molecular profile. These findings reinforce the possibility that the p53 abnormality plays an important role in the carcinogenic mechanism of GAS. Even in cases 8 and 12, where

there were no *TP53* variants, abnormal p53 immunostaining was observed, suggesting loss of *TP53* function and stabilization of the p53 protein in cases 8 and 12, respectively. In non-small-cell lung cancer, overexpression of wild-type p53 has been reported to be associated with immunopositivity of p14 (ARF) with low expression of MDM2, suggesting that deregulation of the p53-MDM2-p14 (ARF) pathway is an alternative pathway [20]. However, no variants in *CDKN2A*, which encodes p14 (ARF) or *MDM2*, were found in case 12. In case 13, we found *MDM2* amplification, which can suppress the function of p53, and *TP53* was indeed co-altered. Interestingly, p53 was overexpressed, and co-alteration of *TP53* with *MDM2* amplification suggests a noncanonical, p53-independent effect for *MDM2* in tumorigenesis. A significant correlation has been reported between tumors containing protein alterations and a poor prognosis [21].

Fig. 2. Summary of genomic alterations and signatures categorized by gene function and signaling pathway in patients with GAS. In the top row, the type of assay and genomic signatures including microsatellite instability, tumor mutational burden, and immunohistochemistry for p53 per case are shown. Genes not analyzed in the CHPv2 assay have a white background. The column on the right represents the total number of alterations per gene. Abbreviations: CHPv2, Cancer Hotspot Panel v2; F1CDx, FoundationOne companion diagnostic; MSI, microsatellite instability; TMB, tumor mutational burden; IHC, immunohistochemistry; N/A, not available; CNV, copy number variation.

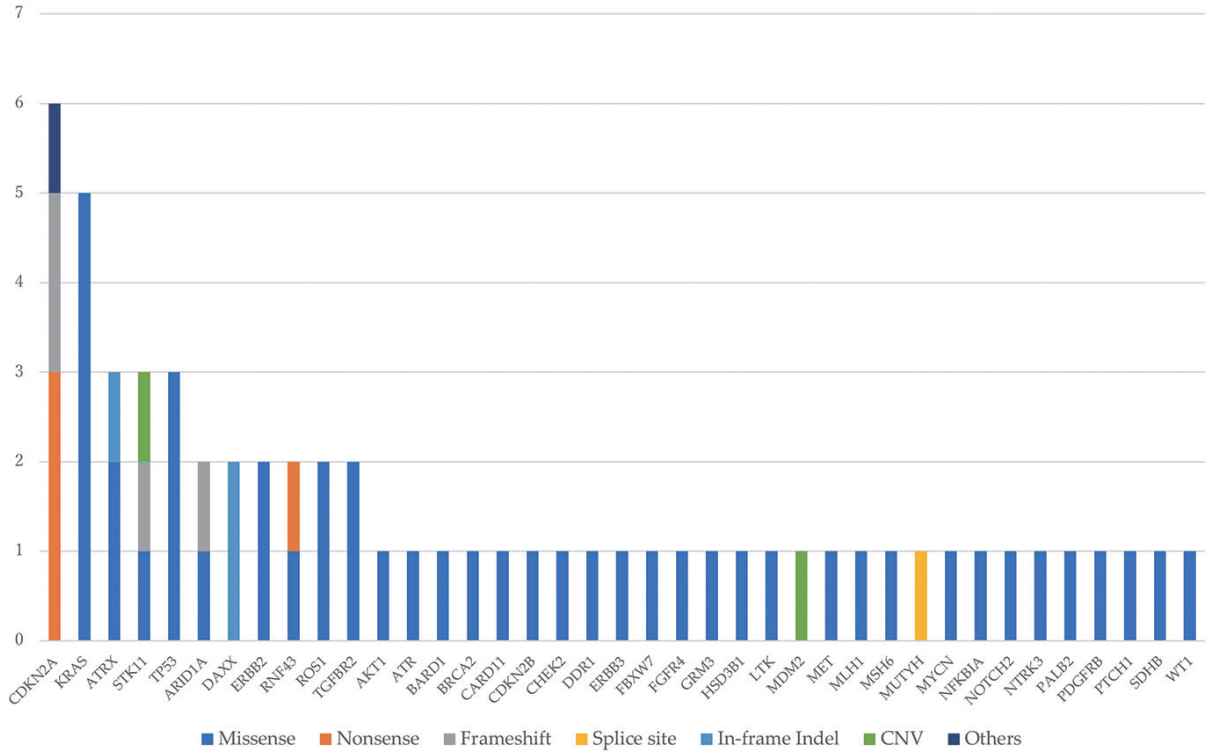

Fig. 3. Distribution of genomic alterations across 6 cases with GAS analyzed by the F1CDx (cases 8–13)

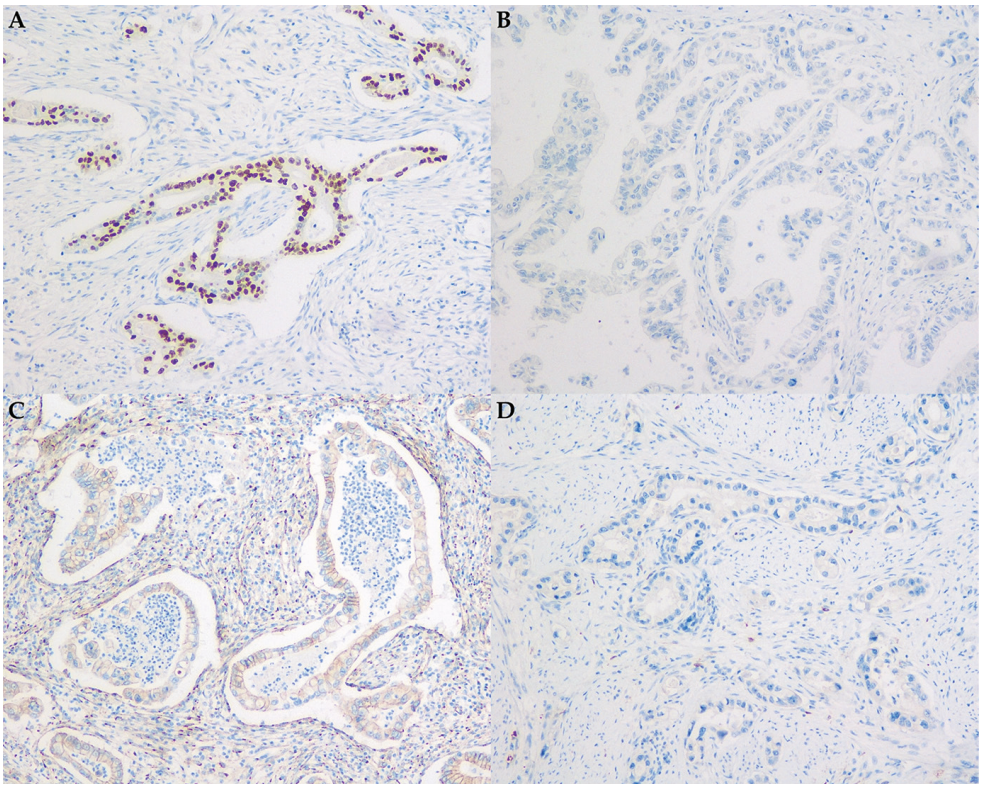

Fig. 4. Immunohistochemical findings of gastric-type mucinous carcinoma with specific molecular profile. (A) p53 overexpression with *TP53* missense variant (case 3). (B) p53 complete absence with *TP53* frameshift variant (case 1). (C) Negative for nuclear β-catenin with *APC* frameshift variant (case 6). (D) Negative for p16 with high-risk HPV negative (case 5).

HPV negativity was observed in all cases except case 13 (HPV type 52), and diffuse positive expression of p16 was not observed in any case. Usually, GAS is negative for p16, a surrogate marker for high-risk HPV infection [4,22]. Case 13 was negative for p16, suggesting that HPV was detected incidentally. These results suggest that even when HPV is present, GAS development follows an HPV-independent path-

TABLE 2.
Summary of the genomic findings

Case	Number of variants	Genomic findings
1	1	*TP53* p.N210Tfs*37
2	1	*TP53* p.R175H
3	3	*APC* p.P1443del, *CDKN2A* p.D108Y, *TP53* p.N239D
4	1	*KRAS* p.G12D
5	3	*APC* p.L1488Ffs*26, *KIT* p.M541L, *TP53* p.R248Q
6	3	*APC* p.L1488Ffs*26, *PIK3CA* p.E453K, *TP53* p.V157F
7	2	*PIK3CA* p.Q60*, *TP53* c.376-1G>A (splice site)
8	9	*ATRX* p.E1021D, *CDKN2A* p.R58*, *CDKN2B0* p.R73G, *MSH6* p.S664A, *MYCN* p.G309V, *NOTCH2* p.D1042G, *PALB2* p.E837K, *PTCH1* p.Y446S, *WT1* p.P249T
9	11	*AKT1* p.T433S, *ATRX* p.S1992del, *BARD1* p.S186G, *CARD11* p.T670M, *CDKN2A* rearragement intron 1, *DAXX* p.E457del, *ERBB2* p.S310Y, *KRAS* p.Q61H, *MUTYH* c.892-2A>G (splice site), *SDHB* p.S163F, *TP53* p.R282W
10	11	*BRCA2* p.V2109I, *CDKN2A* p.L65fs*49, *CHEK2* p.R181H, *DDR1* p.T292M, *ERBB2* p.R678Q, *FBXW7* p.G517E, *HSD3B1* p.H93Q, *KRAS* p.G12V, *RNF43* p.R330*, *STK11* p.S325fs*35, *TGFBR*2 p.C394F
11	8	*CDKN2A* p.L97fs*49, *CDKN2A* p.W15*, *DAXX* p.E457del, *KRAS* p.G13D, *MLH1* p.I32V, *PDGFRB* p.V221M, *STK11* p.Q302P, *TP53* p.Y236C
12	14	*ARID1A* p.A41V, *ARID1A* p.D1850fs*4, *ATR* p.T2556S, *ATRX* p.I574V, *ERBB3* p.G284R, *FGFR4* p.H673R, *KRAS* p.G12D, *KRAS* p.G12S, *LTK* p.L579P, *MET* p.T230M, *NTRK3* p.S552L, *ROS1* p.W133R, *STK11* loss, *TGFBR2* p.S46R
13	7	*CDKN2A* p.Y129*, *GRM3* p.Y478F, *MDM2* amplification, *NFKBIA* p.E282Q, *RNF43* p.S476R, *ROS1* p.W133R, *TP53* p.R248W

TABLE 3.
Relationship between molecular profiles and immunophenotype

Case	*TP53*	p53 IHC	*APC*	nuclear β-catenin IHC	HPV genotyping	p16 IHC
1	Frameshift	Complete absence	WT	Negative	Negative	Negative
2	Missense	Overexpression	WT	Negative	Negative	Negative
3	Missense	Overexpression	In-frame indel	Negative	Negative	Negative
4	WT	Normal expression	WT	Negative	Negative	Negative
5	Missense	Overexpression	Frameshift	Negative	Negative	Negative
6	Missense	Overexpression	Frameshift	Negative	Negative	Negative
7	Splice site	Overexpression	WT	Negative	Negative	Negative
8	WT	Complete absence	WT	Negative	Negative	Negative
9	Missense	N/A	WT	N/A	Negative	N/A
10	WT	Normal expression	WT	N/A	Negative	Negative
11	Missense	Overexpression	WT	N/A	Negative	Negative
12	WT	Overexpression	WT	N/A	Negative	N/A
13	Missense	Overexpression	WT	N/A	52	Negative

Abbreviations: IHC, immunohistochemistry; HPV, human papillomavirus; WT, wild-type; indel, insertion/deletion.

way. However, a small subset of GAS has been reported to show diffuse positive expression even when negative for high-risk HPV [4]. Therefore, when p16 is diffuse positive in GAS, molecular HPV testing should be performed to confirm HPV independence.

CDKN2A was the second most altered gene, with five of the seven alterations being nonsense and frameshift variants that can lead to loss of function. *CDKN2A* encodes two distinct tumor-suppressor proteins: p16 (INK4a), a cyclin-dependent kinase inhibitor, and p14 (ARF), which binds the p53-stabilizing protein MDM2. Both proteins are involved in cell cycle regulation, the RB1 pathway for p16 (INK4a), and the p53 pathway for p14 (ARF). *CDKN2A* loss has been reported to be an important event in many carcinomas, most of which is due to loss-of-function mutation or inactivation by homozygous deletions. Similar to the findings of this study, *CDKN2A* alterations have been reported recurrently in GAS, suggesting that it plays a significant role in the GAS carcinogenesis [10–14]. No *CDKN2A* alterations were reported in ECA (n = 27) in the publicly available data from the cBioportal for Cancer Genomics (http://cbioportal.org). Therefore, *CDKN2A* alterations were considered to be the specific genomic profile characterizing GAS. Most GAS with *CDKN2A/B* variants have been reported to show null p53 expression [10]. However, only case 8 showed negative p53 expression in six cases with *CDKN2A* alterations. Case 8 had wild-type *TP53*, and cases with the coexistence of *CDKN2A* and *TP53* showed p53 overexpression. p14, which is the *CDKN2A* encoded protein, blocks the MDM2-induced degradation of p53. Therefore, the *CDKN2A* loss increases the p53 degradation, which results in a null p53 expression in wild-type *TP53*. The coexistence of *TP53* and *CDKN2A* alterations could lead to p53 overexpression.

Six missense variants were found in *KRAS*, including G12D, G12V, G12S, G13D, and Q61H, all pathological mutations. *KRAS* is associated with the RAS/MAPK signaling pathway and is a critical oncogene reported in various carcinomas, including pancreatic, colorectal, and endometrial cancers. *KRAS* alterations are dominated by missense variants and mainly located in codons 12 and 13. In our study, *KRAS* mutations overlapped with *TP53* and *CDKN2A* alterations, suggesting that these alterations cooperate in pathogenesis. Patients with co-occurrence of *KRAS* G12D with *TP53* alteration have reported to confer better survival than those with any other *KRAS* subtype with *TP53* alteration in pancreatic ductal adenocarcinoma [23]. However, cases 4 and 8 harboring *KRAS* G12D had wild-type *TP53*, and the prognosis was poor. Although *KRAS* mutation has been considered undruggable for decades, sotorasib, a *KRAS* G12C inhibitor, was recently approved for *KRAS* G12C mutated non-small lung cancer [24].

We identified two frameshift and one indel *APC* variants, which occurred at codons 1443 and 1448, part of a region of codons known as the mutation cluster region (codons 1281–1556). Variants associated with sporadic colorectal cancer are frequently found in this region [25–27]. In most colorectal cancers, biallelic *APC* inactivation due to truncation or loss of heterogeneity has been identified, leading to the triggering of tumor development [27]. APC protein truncation caused by frameshift variants may affect the stabilization of β-catenin due to impaired degradation, resulting in aberrant nuclear staining for β-catenin, but β-catenin expression was limited to membranes in our case. Although biallelic *APC* inactivation does not always result in β-catenin nuclear translocation, it may explain our findings show that the *APC* variant was limited to one allele while the intact APC protein was present [28]. High rates of genetic and epigenetic alterations of the APC/β-catenin pathway have been reported in endometrial cancer, but no *APC* variants have been reported in cervical cancer [29].

We identified three *STK11* alterations, two of which were *STK11* loss and frameshift variants, leading to loss-of-function alterations. *STK11* is a tumor-suppressor gene that encodes a serine/threonine kinase that controls the activity of AMP-activated protein kinase family members and is involved in cell polarity, metabolism, apoptosis, and DNA damage response. Alterations in *STK11* have been found, especially in lung adenocarcinoma. *STK11* variants have been repeatedly reported in GAS [10,15,30]. *STK11* is the causative gene of PJS, which is characterized by the association of hamartomatous polyposis of the gastrointestinal tract, mucocutaneous pigmentation, and cancer predisposition, including gastrointestinal, pancreatic, breast, ovarian, and uterine cancers, with 9% of patients developing MDA [31–33]. MDA is an extremely well-differentiated adenocarcinoma that shows the gastric phenotype and is considered to belong to the extremely well-differentiated section of the GAS spectrum [3]. MDA and SCTAT have been reported as gynecologic tumor characteristics of PJS [33]. There were no clinical features suggestive of PJS in three cases with *STK11* alterations. Interestingly, in case 8, we observed the coexistence of MDA with SCTAT and suspected PJS, but a close examination of the gastrointestinal tract revealed no abnormalities or

variants in *STK11*, suggesting epigenetic inactivation [34]. *STK11* variants have been identified in MDA associated with PJS as well as sporadic MDA, suggesting that these genes are characteristic of the GAS phenotype [30,35]. In sporadic cases of GAS, patients with GAS who harbored *STK11* variants had poorer prognosis than those who harbored wild-type *STK11* [30].

Lobular endocervical glandular hyperplasia (LEGH) is a benign lesion that exhibits gastric differentiation, while atypical LEGH and gastric-type adenocarcinoma in situ (gAIS) have been advocated as potential precursors of GAS [3,36,37]. Precursor lesions of GAS, including atypical LEGH and gAIS, have not yet been reported via genetic analyses, while mutually exclusive genetic variants in *GNAS, KRAS*, and *STK11* have been identified in 19 LEGH cases [38]. The *STK11* mutation has only been identified in MDA and not in LEGH [35]. Co-alteration of *KRAS* and *STK11* was observed in our study, suggesting multistep carcinogenesis through the accumulation of genetic aberrations in GAS. Although no *GNAS* variants were found in this study, they have been found in GAS and several types of low-grade gastrointestinal tumors, frequently showing a gastric-type phenotype [12]. *GNAS* variants have also been reported in HPV positive ECA and GAS, suggesting the existence of UEA with *GNAS* variants [15,38].

There were some limitations to this study. First, we used CHPv2 in cases 1 to 8, which only covers about 2800 COSMIC mutations from 50 representative cancer-associated genes, but does not cover genes such as *MSH6, MSH2*, and *BRCA2*, which have been reported in other studies [10,15]. In contrast, in cases 8–13, F1CDx was used not only to perform comprehensive genomic profiling of 324 genes, including the mismatch repair (MMR)- and homologous recombination deficiency (HRD)-related genes mentioned above, but also to determine MSI and calculate the TMB. Because it is inappropriate to simply integrate and interpret the results of the two different assays, the details of the CHPv2 and F1CDx results were presented separately, with F1CDx as the main result and CHPv2 as the supplementary result. Careful attention was paid when integrating the results of two assays. Second, we only included patients who had undergone surgery, except case 12, in which heavy-ion radiotherapy was administered. Due to the relatively small number of cases compared to previous studies, there may be selection bias in the patient's background, which affects the reliability of the results to some extent. Finally, this study was conducted using only pretreatment specimens from the primary site and intratumor genetic heterogeneity was not investigated.

CONCLUSIONS

GAS may represent a group of genetically diverse tumors caused by various genomic alterations associated with sustained activation of signaling pathways or cell cycle regulation, in addition to abnormalities in *TP53*. Co-alteration of various genes, including *TP53, KRAS, CDKN2A*, and *STK11*, was observed, suggesting multistep carcinogenesis through the accumulation of genetic aberrations in patients with GAS. Notably, *CDKN2A* and *STK11* alterations were characteristics of GAS. To our knowledge, this is the first Japanese study of GAS that included comprehensive molecular profiling using FFPE and fresh-frozen specimens. No MSI or TMB-high tumors, which are indications for immune checkpoint inhibitors, were observed. Although not found in this study, genetic variants involved in MMR and HRD—predictive markers for the immune checkpoint inhibitor and poly (ADP-ribose) polymerase inhibitor responses—have been reported [10]. Circulating tumor DNA analysis, which involves noninvasive NGS-based liquid biopsy, has emerged as a promising tool that can be used for early tumor diagnosis and to determine tumor heterogeneity due to genetic changes during cancer treatment [39–41]. Although its use in GAS has not yet been reported, it is expected to be effective. We did not find any MBRTs in this study. However, precision medicine based on molecular profiles seems necessary to overcome the aggressive nature of GAS.

DECLARATIONS

AUTHOR CONTRIBUTIONS: Conceptualization, H.N., S.N. and K.K.; methodology, H.N. and S.N.; software, H.N.; validation, S.N., N.T. and K.K.; formal analysis, H.N., N.T. and K.K.; investigation, H.N., N.T. and K.K.; resources, H.N., J.P., K.T., A.T., S.N., N.T., S.K-S., J.A. and K.K.; data curation, S.N.; writing—original draft preparation, H.N.; writing—review and editing, all authors; visualization, H.N.; supervision, S.N. and K.U.; project administration, K.U.; funding acquisition, H.N. and K.U. All authors have read and agreed to the published version of the manuscript.

FUNDING: This study was funded by the Supporting Fund of Obstetrics and Gynecology of Kurume University and Young Researchers Grant of Research Center for Innovative Cancer Therapy, Kurume University.

INSTITUTIONAL REVIEW BOARD STATEMENT: The study was conducted in accordance with the Declaration of Helsinki and approved by the Ethical Committee of Kurume

University (study ID: 387 and date of approval: January 28, 2019).

INFORMED CONSENT STATEMENT: Informed consent was obtained from all patients included in the study.

DATA AVAILABILITY STATEMENT: The study data are only available on request due to privacy/ethical restrictions.

ACKNOWLEDGMENTS: The authors are grateful to all the patients who participated in this study. We thank Editage (www.editage.com) for English editing.

CONFLICTS OF INTEREST: The authors declare no conflict of interest.

REFERENCES

1. Kurman RJ, Carcangiu ML, Harrington CS, and Young RH. WHO Classification of Tumours of Female Reproductive Organs. IARC Press 2014; 6:307.
2. Kojima A, Mikami Y, Sudo T, Yamaguchi S, Kusanagi Y et al. Gastric morphology and immunophenotype predict poor outcome in mucinous adenocarcinoma of the uterine cervix. Am J Surg Pathol 2007; 31:664-672.
3. Mikami Y, Kiyokawa T, Hata S, Fujiwara K, Moriya T et al. Gastrointestinal immunophenotype in adenocarcinomas of the uterine cervix and related glandular lesions: A possible link between lobular endocervical glandular hyperplasia/pyloric gland metaplasia and 'adenoma malignum'. Mod Pathol 2004; 17:962-972.
4. Carleton C, Hoang L, Sah S, Kiyokawa T, Karamurzin YS et al. A detailed immunohistochemical analysis of a large series of cervical and vaginal gastric-type adenocarcinomas. Am J Surg Pathol 2016; 40:636-644.
5. Kusanagi Y, Kojima A, Mikami Y, Kiyokawa T, Sudo T et al. Absence of high-risk human Papillomavirus (HPV) detection in endocervical adenocarcinoma with gastric morphology and phenotype. Am J Pathol 2010; 177:2169-2175.
6. Holl K, Nowakowski AM, Powell N, McCluggage WG, Pirog EC et al. Human papillomavirus prevalence and type-distribution in cervical glandular neoplasias: Results from a European multinational epidemiological study. Int J Cancer 2015; 137:2858-2868.
7. Karamurzin YS, Kiyokawa T, Parkash V, Jotwani AR, Patel P et al. Gastric-type endocervical adenocarcinoma: An aggressive tumor with unusual metastatic patterns and poor prognosis. Am J Surg Pathol 2015; 39:1449-1457.
8. Nishio S, Mikami Y, Tokunaga H, Yaegashi N, Satoh T et al. Analysis of gastric-type mucinous carcinoma of the uterine cervix — An aggressive tumor with a poor prognosis: A multi-institutional study. Gynecol Oncol 2019; 153:13-19.
9. Kojima A, Shimada M, Mikami Y, Nagao S, Takeshima N et al. Chemoresistance of gastric-type mucinous carcinoma of the uterine cervix: A study of the sankai gynecology study group. Int J Gynecol Cancer 2018; 28:99-106.
10. Garg S, Nagaria TS, Clarke B, Freedman O, Khan Z et al. Molecular characterization of gastric-type endocervical adenocarcinoma using next-generation sequencing. Mod Pathol 2019; 32:1823-1833.
11. Selenica P, Alemar B, Matrai C, Talia KL, Veras E et al. Massively parallel sequencing analysis of 68 gastric-type cervical adenocarcinomas reveals mutations in cell cycle-related genes and potentially targetable mutations. Mod Pathol 2021; 34:1213-1225.
12. Hodgson A, Howitt BE, Park KJ, Lindeman N, Nucci MR et al. Genomic characterization of HPV-related and gastric-type endocervical adenocarcinoma: Correlation with subtype and clinical behavior. Int J Gynecol Pathol 2020; 39:578-586.
13. Jung H, Bae GE, Kim HM, and Kim HS. Clinicopathological and molecular differences between gastric-type mucinous carcinoma and usual-type endocervical adenocarcinoma of the uterine cervix. Cancer Genomics Proteomics 2020; 17:627-641.
14. Lu S, Shi J, Zhang X, Kong F, Liu L et al. Comprehensive genomic profiling and prognostic analysis of cervical gastric-type mucinous adenocarcinoma. Virchows Arch 2021; 479:893-903.
15. Park E, Kim SW, Kim S, Kim HS, Lee JY et al. Genetic characteristics of gastric-type mucinous carcinoma of the uterine cervix. Mod Pathol 2021; 34:637-646.
16. Frampton GM, Fichtenholtz A, Otto GA, Wang K, Downing SR et al. Development and validation of a clinical cancer genomic profiling test based on massively parallel DNA sequencing. Nat Biotechnol 2013; 31:1023-1031.
17. Kawano K, Tsuda N, Waki K, Matsueda S, Hata Y et al. Personalized peptide vaccination for cervical cancer patients who have received prior platinum-based chemotherapy. Cancer Sci 2015; 106:1111-1117.
18. Sasagawa T, Maehama T, Ideta K, Irie T, and Fujiko Itoh J-HERS Study Group. Population-based study for human papillomavirus (HPV) infection in young women in Japan: A multicenter study by the Japanese human papillomavirus disease education research survey group (J-HERS). J Med Virol 2016; 88:324-335.
19. Oren M and Rotter V. Mutant p53 gain-of-function in cancer. Cold Spring Harb Perspect Biol 2010; 2:a001107.
20. Wang YC, Lin RK, Tan YH, Chen JT, Chen CY et al. Wild-type p53 overexpression and its correlation with MDM2 and p14ARF alterations: An alternative pathway to non-small-cell lung cancer. J Clin Oncol 2005; 23:154-164.
21. Cordon-Cardo C, Latres E, Drobnjak M, Oliva MR, Pollack D et al. Molecular abnormalities of mdm2 and p53 genes in adult soft tissue sarcomas. Cancer Res 1994; 54:794-799.
22. Keating JT, Cviko A, Riethdorf S, Riethdorf L, Quade BJ, Sun D et al. Ki-67, cyclin E, and p16INK4 are complimentary surrogate biomarkers for human papilloma virus-related cervical neoplasia. Am J Surg Pathol 2001; 25:884-891.
23. Shoucair S, Habib JR, Pu N, Kinny-Köster B, van Ooston AF et al. Comprehensive analysis of somatic mutations in driver genes of resected pancreatic ductal adenocarcinoma reveals KRAS G12D and mutant TP53 combination as an independent predictor of clinical outcome. Ann Surg Oncol 2022; 29:2720-2731.
24. Huang L, Guo Z, Wang F, and Fu L. KRAS mutation: From undruggable to druggable in cancer. Signal Transduct Target Ther 2021; 6:386.

25. Miyoshi Y, Nagase H, Ando H, Horii A, Ichii S et al. Somatic mutations of the APC gene in colorectal tumors: Mutation cluster region in the APC gene. Hum Mol Genet 1992; 1:229-233.
26. Cheadle JP, Krawczak M, Thomas MW, Hodges AK, Al-Tassan N et al. Different combinations of biallelic APC mutation confer different growth advantages in colorectal tumours. Cancer Res 2002; 62:363-366.
27. Rowan AJ, Lamlum H, Ilyas M, Wheeler J, Straub J et al. APC mutations in sporadic colorectal tumors: A mutational "hotspot" and interdependence of the "two hits". Proc Natl. Acad Sci U S A 2000; 97:3352-3357.
28. Bläker H, Scholten M, Sutter C, Otto HF, and Penzel R. Somatic mutations in familial adenomatous polyps: Nuclear translocation of β-catenin requires more than biallelic APC inactivation. Am J Clin Pathol 2003; 120:418-423.
29. Moreno-Bueno G, Hardisson D, Sánchez C, Sarrió D, Cassia R et al. Abnormalities of the APC/β-catenin pathway in endometrial cancer. Oncogene 2002; 21:7981-7990.
30. Kuragaki C, Enomoto T, Ueno Y, Sun H, Fujita M et al Mutations in the STK11 gene characterize minimal deviation adenocarcinoma of the uterine cervix. Lab Invest 2003; 83:35-45.
31. Hemminki A, Markie D, Tomlinson I, Avizienyte E, Roth S et al. A serine/threonine kinase gene defective in Peutz-Jeghers syndrome. Nature 1998; 391:184-187.
32. Bosman FT. The hamartoma-adenoma-carcinoma sequence. J Pathol 1999; 188:1-2.
33. Banno K, Kisu I, Yanokura M, Masuda K, Ueki A et al. Hereditary gynecological tumors associated with Peutz-Jeghers syndrome (Review). Oncol Lett 2013; 6:1184-1188.
34. Esteller M, Avizienyte E, Corn PG, Lothe RA, Baylin SB et al. Epigenetic inactivation of LKB1 in primary tumors associated with the Peutz-Jeghers syndrome. Oncogene 2000; 19:164-168.
35. Takatsu A, Miyamoto T, Fuseya C, Suzuki A, Kashima H et al. Clonality analysis suggests that STK11 gene mutations are involved in progression of lobular endocervical glandular hyperplasia (LEGH) to minimal deviation adenocarcinoma (MDA). Virchows Arch 2013; 462:645-651.
36. Talia KL, Stewart CJR, Howitt BE, Nucci MR, and McCluggage WG. HPV-negative gastric type adenocarcinoma in situ of the cervix: A spectrum of rare lesions exhibiting gastric and intestinal differentiation. Am J Surg Pathol 2017; 41:1023-1033.
37. Kawauchi S, Kusuda T, Liu XP, Suehiro Y, Kaku T et al. Is lobular endocervical glandular hyperplasia a cancerous precursor of minimal deviation adenocarcinoma?: A comparative molecular-genetic and immunohistochemical study. Am J Surg Pathol 2008; 32:1807-1815.
38. Matsubara A, Sekine S, Ogawa R, Yoshida M, Kasamatsu T et al. Lobular endocervical glandular hyperplasia is a neoplastic entity with frequent activating GNAS mutations. Am J Surg Pathol 2014; 38:370-376.
39. Rodriguez BJ, Córdoba GD, Aranda AG, Álvarez M, Vicioso L et al. Detection of TP53 and PIK3CA mutations in circulating tumor DNA using next-generation sequencing in the screening process for early breast cancer diagnosis. J Clin Med 2019; 8:1183.
40. Parikh AR, Leshchiner I, Elagina L, Goyal L, Levovitz C et al. Liquid versus tissue biopsy for detecting acquired resistance and tumor heterogeneity in gastrointestinal cancers. Nat Med 2019; 25:1415-1421.
41. Rodríguez-Casanova A, Bao-Caamano A, Lago-Lestón RM, Brozos-Vázquez E, Costa-Fraga N et al. Evaluation of a targeted next-generation sequencing panel for the non-invasive detection of variants in circulating DNA of colorectal cancer. J Clin Med 2021; 10:4487.

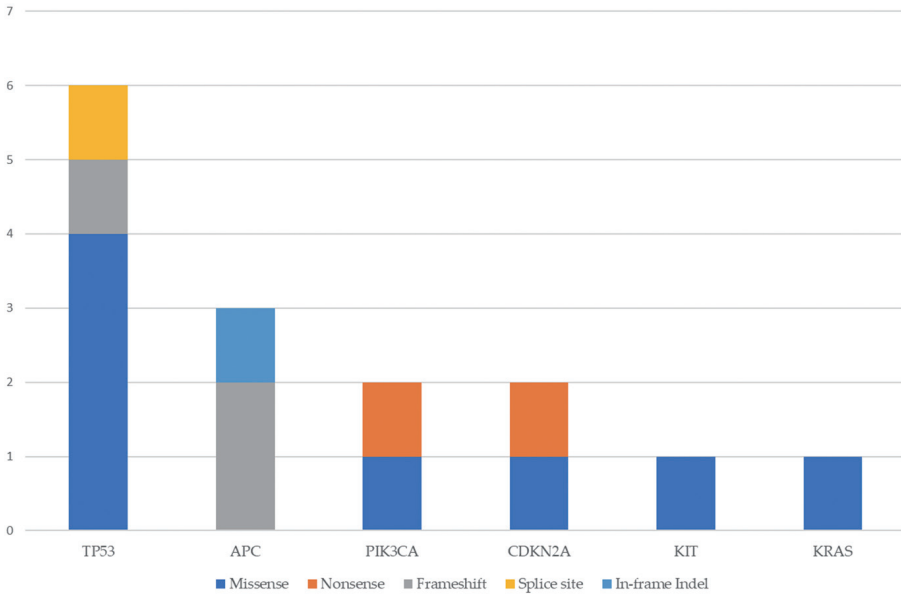

Supplementary Figure 1S. Distribution of genomic alterations across 8 cases with GAS analyzed by the CHPv2 (cases 1–8)